

HOSTED BY



ELSEVIER

Contents lists available at ScienceDirect

Engineering Science and Technology, an International Journal

journal homepage: www.elsevier.com/locate/jestch

Full Length Article

Fabrication and characterization of zeolite coatings on aluminum and magnesium alloys

Giovanna Rotella^{a,*}, Sebastiano Candamano^b^a Department of Informatics, Modeling, Electronics and Systems Engineering (DIMES), University of Calabria, Rende, CS 87036, Italy^b Department of Mechanical, Energy and Management Engineering, University of Calabria, Rende, CS 87036, Italy

ARTICLE INFO

Article history:

Received 7 January 2020

Revised 18 February 2020

Accepted 18 March 2020

Available online xxx

Keywords:

Coatings fabrication

Adhesion test

Scratch test

Aluminum

Magnesium

ABSTRACT

This work presents a methodology to fabricate zeolite coating on aluminum and magnesium alloys. A procedure for coating AA 6082 aluminum and AZ31B magnesium alloys substrates with a homogeneous, adherent and anticorrosive layer of a zeolite filler embedded in a silane matrix is developed. The adhesion of the coating has been probed by scratch and shear tests. Furthermore, the coating strength at high strain rate has been tested by tensile impact testing method. Also, the corrosion resistance of the coated samples has been verified highlighting an improvement with respect to the uncoated materials. The overall results show a very good surface coverage grade and a good level of coating adhesion and strength.

© 2020 Karabuk University. Publishing services by Elsevier B.V. This is an open access article under the CC BY-NC-ND license (<http://creativecommons.org/licenses/by-nc-nd/4.0/>).

1. Introduction

Coating is one of the most commonly adopted techniques used as protective layers for metals. The nature of the coating strongly depends on the protection needed (corrosion, wear, heat etc. . .), whereas its durability and reliability depend on its adhesion to the substrate, which is, most of the time, difficult to achieve [1–5]. Thus, it is important to choose constituents having good chemical affinity to the metal substrate or, alternatively, to enhance the adhesive properties of the substrate by surface modifications [6–8]. Furthermore, the stricter market rules of having highly reliable multifunctional materials force researchers and manufacturers to find useful strategies for high performance coatings development. Zeolites are a large group of natural and synthetic crystalline aluminosilicates characterized by a complex three-dimensional framework that can accommodate exchangeable cations [8]. Different studies investigated zeolite coatings on both ceramic and metal surfaces [8–12], operating as catalyst, molecular sieves or sensors [13]. Moreover, as zeolites can operate in harsh environments, are non-toxic and can be used as controlled releasing agents, they can find potential interesting applications, as metal coatings, either with protective aims, such as effective barrier to

corrosive medium and preventing the release of harmful ions. Zeolites thin films and coatings can find many potential industrial applications, as sensor materials, low-k dielectric films, antimicrobial surface coatings, in computer chips, in food and pharmaceutical industries [14–19]. Moreover, the highly regular structure of pores and the presence of extra-framework and exchangeable cations (such as Na⁺, K⁺, Ca²⁺) of zeolites can be also exploited to selectively incorporate specific molecules or ions that act as chemicals or corrosion inhibitors which can then be gradually released during coating service or in presence of relevant conditions of temperature, pH and moisture [20–23]. Several methodologies are adopted to produce zeolites coatings and they are strictly related to metal support chemical composition, geometry and dimensions, type of deposited zeolite, desired coating thickness (that is one of the most important coating characteristics) [24–26]. The *in situ* hydrothermal synthesis of zeolites on metals, for example, allows obtaining good interface properties, but the control of the layer thickness is difficult to be achieved, the pH of the reactive medium is often corrosive for the metals and dimension/shape of the supports that can be useful processed is limited [27]. The above-mentioned disadvantages can be overcome by dip-coating technology, once the proper coupling agent or binder and metals surface treatments are identified.

The aim of this work is thus to implement a procedure for coating AA 6082 aluminum and AZ31B magnesium alloys substrates with a homogeneous, adherent and anticorrosive layer consisting of a zeolite filler embedded in a silane matrix.

* Corresponding author.

E-mail addresses: giovanna.rotella@unical.it (G. Rotella), sebastiano.candamano@unical.it (S. Candamano).

Peer review under responsibility of Karabuk University.

<https://doi.org/10.1016/j.jestch.2020.03.008>

2215-0986/© 2020 Karabuk University. Publishing services by Elsevier B.V.

This is an open access article under the CC BY-NC-ND license (<http://creativecommons.org/licenses/by-nc-nd/4.0/>).

Magnesium alloys are of great interest for the automobile and clinical industries because of their low cytotoxicity, low density, excellent mechanical properties and castability. However, their low resistance to corrosion prevent them from extensive applications [28]. Furthermore, coatings obtained by anodizing, electroplating, conversion coating, vapor phase deposition result to be expensive, hazardous or ineffective [29–31].

AA6082 is characterized by good machinability and weldability and it finds important applications in the automotive sector. It possesses high corrosion resistance, but localized corrosion, such as pitting and intergranular corrosion, sometimes occurs [32,33].

Thus, it is of great interest to find alternative solutions for effectively coat such materials for corrosion prevention [24]. In fact, even though aluminum alloys have been previously treated in order to be coated by zeolites, to authors' knowledge zeolite/silane multifunctional coating has not been applied to Mg alloys.

2. Material and method

The materials under investigation are AA6082 aluminum alloy and AZ31B magnesium alloy. They have been used in the form of metal sheets. The as received surface morphology and the grade of coating coverage were analyzed by Scanning Electron Microscope (SEM) analysis (FEI Company model Inspect). The wettability changes after coating were verified by contact angle measurements using a customized device. In particular, the device was equipped with a Digital Image Correlation (DIC) camera and a calibrated liquid delivery system. The images were processed using a built-in contact angle measurement software. However, in order to verify the accuracy of the applied methodology the contact angles have also been measured by a conventional contact angle measuring device (OCA-20, Data Physics, Germany) equipped with a Charged Coupled Device (CCD) camera with a resolution of 768×576 pixel. The sessile drop technique was applied by delivering a $3 \mu\text{l}$ drop of distilled water placed on probed surfaces and the equilibrium contact angle was determined. Thus, the equilibrium time able to spread capillarity was set equal to 15 s. The overall difference between the measuring devices was considered negligible (average error less than 2%). The performance of the coating on both substrates was also evaluated. In particular, the coating material and the substrates were characterized by nano indentation tests in terms of hardness and Young modulus, while its adhesion was tested by scratch and single lap shear tests.

The substrates were obtained from 1.5 mm thick AA 6082 aluminum and AZ31B magnesium alloys. The metals alloy sheets were cut into $10 \text{ mm} \times 45 \text{ mm}$. All the samples, prior coating, have been manually mechanically polished with progressively finer SiC papers up to 4000 grade and washed with distilled water. Then samples were ultrasonically cleaned using acetone and dried in air. Afterwards, the AA 6082 specimens were ultrasound treated in a 0.1 M NaOH solution for 60 s [6], whereas AZ31B samples in ultrasonic bath in a 3.0 M of NaOH for 2 h [34].

Finally, specimens were rinsed and washed with distilled water and acetone and then dried in air. The aim of the above process is to generate metal hydroxyls groups at the metal surface.

N-Propyl-trimethoxy-silane hydrolysed by ethanol and distilled water (ethanol:H₂O:silane 90:5:5 v/v%) was prepared and its self-condensation tendency was controlled by adjusting the pH level to 4 adding acetic acid. The solution was stirred at room temperature for 24 h to allow hydrolysis to properly proceed. Afterwards, a commercial potassium calcium sodium aluminosilicate of the zeolite A type (commercial name L-Powder by Honeywell UOP) was added to the solution as much as the 90% wt of the silane amount [35]. It has an approximate pore size of 3 Å and a particle size distribution, based on a volume distribution and measured using a Mastersizer 2000 by Malvern Instruments, characterized by a

D10 of 1.56 μm , a D50 of 3 μm and a D90 of 5.4 μm . The selected zeolite is a moisture scavenger for plastics, coating systems and adhesives and its X-ray diffractogram is reported in Fig. 1.

It has been collected on a Rigaku MiniFlex 600 X-ray diffractometer (Rigaku Corporation, Tokyo, Japan) with CuK α , radiation generated at 20 mA and 40 KV. Powder has been scanned from 5 to 50° at 0.02 2 θ steps integrated at a rate of 1°/min. The zeolite was dispersed in the solution and magnetically stirred for 10 min, and then it was placed in an ultrasonic bath for 20 min and subsequently stirred for other 20 min.

The dip coating procedure has been performed at different immersion, start-up and withdrawing rates to verify the coating homogeneity and thickness. In fact, even though the silane molecules link very fast onto the metal surface, the homogeneity and coverage rate can be affected by the immersion time as demonstrated by Ref. [6]. Thus, the selected immersion rate was of 1 mm/s, the start-up was fixed to 1 min and the withdrawing rate was set to 1 mm/s. The final layer thickness was of about 20 μm and it was obtained by two dip coating stages. The first one was performed at 1 mm/s immersion rate and 1 min of start-up with a subsequent withdrawing rate of 1 mm/s. The so obtained surfaces were cured at 80 °C for 30 min. A second step of dip coating was executed with the same parameters as the previous stage and then cured at 80 °C for 3 h to provide a final high crosslinking degree of the silane [36].

SEM images of the as received and the coated samples have been acquired in order to verify the surface morphology prior and after coating as well as the surface coverage grade (CG).

The adhesion strength of the coating on the metal substrates has been tested with different methodologies. Based on the nanoindentation results, scratch tests have been performed at progressive load over the coating to determine the critical loads for coating delamination. Also, other batches of coated samples have been cut into $25 \times 100 \text{ mm}$, bonded using an epoxy resin and tested under shear load, at low and high strain rates, to verify the adhesion strength of the coating when a bigger area is involved. Fig. 2 reports a schematic of the lap shear and impact samples. In particular, the ASTM D1200 has been followed for testing the specimens. The samples were bonded using a dual component epoxy resin curing at room temperature for 24 h as suggested by the manufacturer. The overlap length has been set to be 12.5 mm while the substrates thickness was of 1.5 mm and the width of 25 mm. The tensile tests were performed using an electromechanical testing machine with the cross-head speed set equal to 1 mm/min. Ten joint were bonded and tested for each material. The average shear strength is defined and calculated as:

$$\tau_a = \frac{P_{max}}{A}$$

where P_{max} is the maximum registered load and A is the bond area.

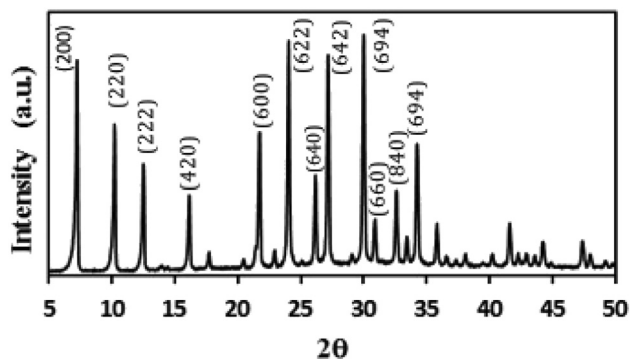


Fig. 1. X-ray diffractogram of Commercial Zeolite [PDF 00-043-0142]

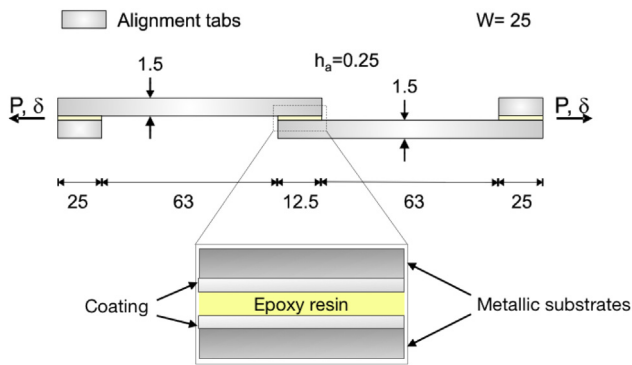


Fig. 2. Schematic of the Single Lap Joint and Impact tests (all the reported measures are in mm).

The shear strength of the coating/substrate under high strain rate was probed by a tensile impact test device (*Instron CEAST 9350*) to quantify the impact energy necessary to remove the coating from the substrate. The impact test consisted in hitting the single lap samples by a drop weight allowed to freely fall down from different heights. The sample was placed on a proper support reproducing the configuration explained for the static tests. In particular, the overall mass weight was declared to be 3.49 kg falling from a height of 204 mm registering a speed at impact of 2 m/s. After impact, the specimens were removed and the fracture surfaces were observed in order to verify the failure mechanism.

Finally, the samples have been tested for corrosion resistance in 5% NaCl solution in accordance with ASTM B895. All the tests have been repeated for at least 5 times in order to ensure statistical validity.

3. Results and discussion

The morphology of the coating has been mainly analyzed by means of SEM inspections (via secondary electron microscopy) as reported in Fig. 3. Coatings on both aluminum and magnesium alloys exhibited a quite homogeneous and regular surface revealing a successful coating procedure. A minimum amount of voids is also shown in the SEM figures that allows to highlight the layered nature of the coating. The images also show the zeolite crystallites embedded in the silane matrix. Furthermore, some agglomeration of the zeolite domains led to the formation of zeolite micelles which can be considered weak places prone to detach easier than the rest of the coating.

Fig. 3 also depicts the coverage grade of the coating calculated by processing the SEM images with the software *ImagePro plus*. For both Aluminum and Magnesium alloys the coverage grade was good and it was measured to be more than the 90% for the AA 6082 and about 89% for the AZ31B, suggesting a good selection of the dip coating process parameters as well as a good surface

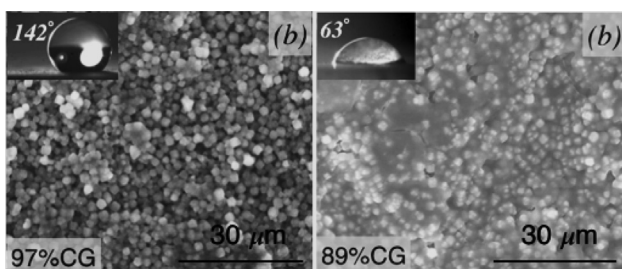


Fig. 3. SEM images of (a) coated Aluminum and (b) Magnesium alloy 3 M NaOH.

pre-treatment and a successful coating solution formulation. Fig. 3 also reports the average contact angle for the considered coated samples. The silane nature is that to increase the hydrophobicity of the metals but, as shown from the results, the coated metals behave differently in terms of wettability. In particular, coated aluminum alloy exhibited a tremendous increase of its hydrophobicity. This indicates that the durability of the metal, in terms of corrosion resistance, can be drastically improved under wet conditions. The reason lies into both morphological and chemical nature of the coating. In fact, the roughness of the microporous coating trapped the air which, accordingly to the Cassie-Baxter theory, increases the apparent contact angle unless the drop is pressed against the surface (Wenzel regime). Furthermore, the presence of external silanol groups (especially of free SiOH groups) on zeolite crystals allow the interaction with the silane matrix favouring the chemical absorption of the silane coupling agents, reducing the hydrophilic OH groups and acquiring hydrophobic organics [37,38]. On the other hands, magnesium alloy become apparently hydrophilic. However, this decrease in contact angle is due to a topography effect. In fact, the pretreatment with NaOH which creates craters over the surfaces increasing the roughness of the material over 1 μm . In fact, the measured R_a for the AA 6082 was probed to be about 3.5 μm (± 0.49) while it was probed to be of about 5.7 μm (± 0.91) for the AZ31B (the measurements were acquired by a contact profilometer on a length of 5 mm and with 10 repetitions). This implies the possibility of the water to fill into the channels generated by the pretreatment drastically decreasing the apparent contact angle that is, in this case, dictated by a morphological change rather than a chemical interaction between the coating and the water drop. Furthermore, the coating thickness resulted homogeneous as also shown in Fig. 4. In particular, the samples have been analyzed along the thickness (Fig. 4(a) and (b)) and, Fig. 4(c) also reports a SEM of the cross section of the coated sample been mounted on a cold curing resin and polished without water up to 9 mm polishing grade in order to better highlight the coating thickness and uniformity.

X-ray diffraction analyses of the zeolite and of the two bare and coated metal substrates, carried out using the conventional symmetrical Bragg Brentano configuration ($\theta/2\theta$) are reported in Figs. 5 and 6.

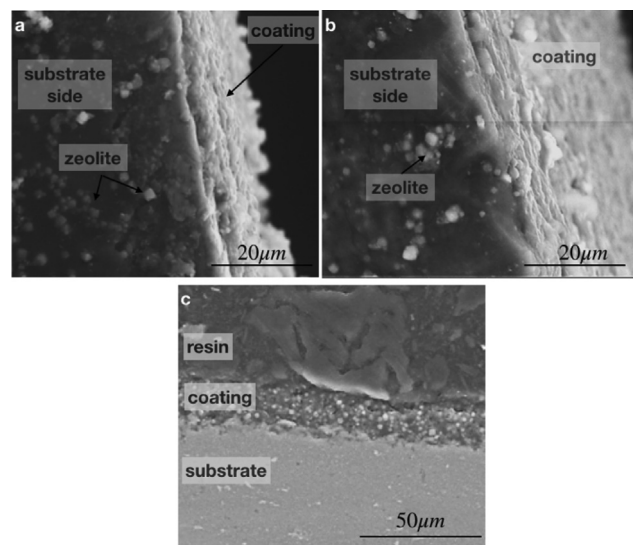


Fig. 4. SEM images of coated cross sections of aluminum (a), (c) and magnesium (b) after the first (a) and the second step (c).

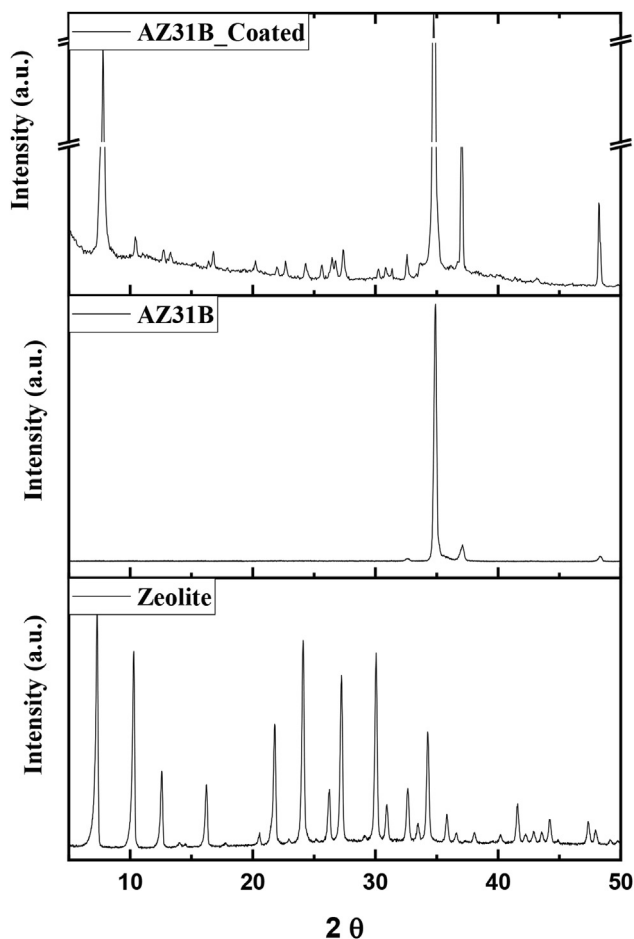


Fig. 5. X-ray diffractogram of bare and coated AZ31B substrate.

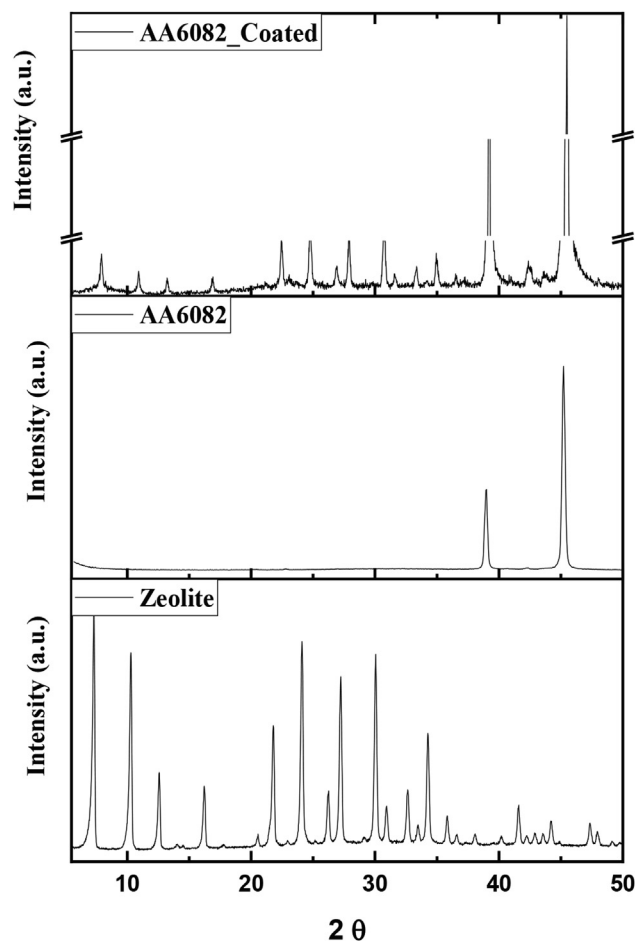


Fig. 6. X-ray diffractogram of bare and coated AA6082 substrate.

The diffractogram of the coated AZ31B substrate (Fig. 5), even showing all the distinctive zeolite peaks, is characterized by a more pronounced (2 0 0) peak, indicating that a more preferred orientation of LTA crystallites with their a-axis perpendicular to the substrate surface exists.

The diffractogram of coated AA6082 substrate (Fig. 6) shows all the peaks that characterize the zeolite diffraction pattern that is typical of a random orientation of its crystallites [38].

The zeolite coating hardness was probed by instrumented nano indentation machine provided with a Berkovich tip. The cross sections of the coated samples were mounted on a cold resin and gently polished in order to obtain a planar smooth surface. Thus, both the coating and the substrate were characterized from the same sample. The nano indentation tests have been carried out at different maximum load and dwell time for the substrates and the silane/zeolite coating. In fact, it is necessary to properly select these parameters according to the material to be tested [39,40]. Preliminary tests have been then carried out in order to select the correct parameters of testing. The maximum load and dwell time were set equal to 10 mN and 10 s respectively for the coating while the aluminum and magnesium alloys have been tested at 20 mN and 15 s. A total of 20 indentations for each material have been performed and the average value has been taken as the Berkovich hardness (HIT) calculated by Oliver and Pharr method. The results highlighted a soft coating over each substrate since the HIT values were probed to be (0.9 ± 0.064) GPa, (1 ± 0.061) GPa and (1.6 ± 0.080) GPa for the L-Powder, AZ31B and AA6082 respectively. Furthermore, the porous origin of the coating turned out into a more difficult estimation of the hardness with consequent higher data dispersion.

The hardness characterization of the zeolite confirmed the soft nature of the coating. Soft coatings (Hardness <5 GPa) usually fail by plastic deformation on softer or harder substrates [41]. Thus, the scratch test can only give qualitative assessment of the coating adhesion unless the interfacial shear stress is less than the shear strength of the coating.

The micro scratch test was performed with a Rockwell tip at a progressive load from 50 mN to 1000 mN at a length of 10 mm. The scratch tester, equipped with optical microscope, allowed to correlate the image of the scratched surface with the corresponding loading value so that the critical load can be identified. Furthermore, in order to clearly identify the area where the coating was completely removed from the substrate, SEM images were also taken after the test.

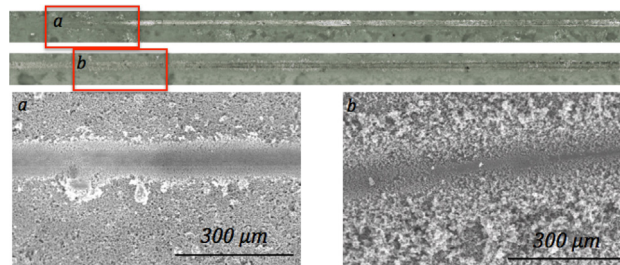


Fig. 7. Scratch test microscopy and SEM of (a) AA6082 and (b) AZ31B samples.

Fig. 7 reports the scratch test results for both AA6082 and AZ31B Mg alloy. The critical load needed to damage the coated surface are identified to be 350 mN for the Aluminum alloy and 400 mN for the Mg alloy. The results highlight similar resistance of the coating over the selected substrates with a slighter increase for the AZ31B. Furthermore, the obtained results show that the concentration of the alkaline solution and the immersion time have to be carefully tuned on selected substrates in order to provide similar quality and the extent of the coating. By varying the concentration of the alkaline solution and the immersion time, comparable amount of hydroxyl groups can be produced on different metal surfaces that can react with hydrolyzed silicon to form hydrogen bond. The following heat treatment allows the formation of Si-O-Mg covalent bond by dehydration.

The adhesive shear strength of the coating was probed using a single-lap-joint test. The overall results highlighted a good adhesion of the coating since the shear strength recorded were 1.8 (± 0.082) MPa for the AZ31B and 1.3 (± 0.065) MPa for the AA 6082. Furthermore, it is worth noting that the failure mechanism always involved the full detachment of the coating from the substrate so that the results could be directly related to their reciprocal adhesion. Also for the dynamic tests, the failure was verified to be adhesive.

The impact tests results recorded a maximum peak load of about 420 (± 24) N and 600 (± 38) N for the coated aluminum and magnesium alloys respectively confirming a slight better adhesion of the zeolite on the Magnesium alloy.

The preliminary corrosion results are shown in Fig. 8 reporting the results for coated and uncoated aluminum and magnesium alloys.

The micrographs reveal a good response of the coating in protecting the substrate. In particular, as expected, the uncoated magnesium alloy exhibited the worst corrosion resistance showing heavy corrosion marks after 30 min. of immersion in the corrosive solution. Also, aluminum alloy revealed the pitting occurrence after 60 min of immersion. On the contrary, the coated magnesium alloy significantly increase the corrosion resistance highlighting the corrosion marks after 240 min of immersion. Finally, the best

results are reported for coated aluminum alloy which last up to 1440 min before showing deterioration marks. Thus, the coating protection effect is noticeable and it is justified by the wettability decrease after the treatment. Also, the results highlight the good bond between the coating and the substrate with a uniform coverage and the absence of voids.

4. Conclusions

A thin homogeneous, adherent and anticorrosive layer consisting of a zeolite filler embedded in a silane matrix was successfully and homogeneously deposited on AA6082 and AZ31B surfaces. Alkaline pre-treatments were optimized to provide adequate hydroxyl groups to metals' surface that acted as attachment points for silane-hydroxy. The presence of silanol groups on zeolite crystals external surface guaranteed the interaction with the silane coupling agent. The selection of appropriate dip coating parameters, such as immersion time, start-up and withdrawing rates, allowed to control coating homogeneity and thickness. The thermal treatment caused the formation of strong Si-O-Mg and Si-O-Al bonds.

The obtained coated surface exhibited a very good coverage grade spanning from 89% to 97%, the contact angle was revealing a different behavior between the substrates even though the coating solution was the same.

The mechanical and chemical characterization of the samples showed a very good adhesion between the coating and the substrates (1.8 MPa and 1.3 MPa for AZ31B and AA6082 respectively) that are essential for further study such as wear resistance. Finally, a good response of the corrosive environment was registered. In fact, corrosion improvements of 8 times for the magnesium alloy and 24 times for the aluminum alloys were registered.

Declaration of Competing Interest

The authors declare that they have no known competing financial interests or personal relationships that could have appeared to influence the work reported in this paper.

References

- [1] M.F. Morks, Fabrication and characterization of plasma-sprayed HA/SiO₂ coatings for biomedical application, *J. Mech. Behav. Biomed. Mater.* (2008), <https://doi.org/10.1016/j.jmbbm.2007.04.003>.
- [2] J.Y. Seok, M. Yang, A novel blade-jet coating method for achieving ultrathin, uniform film toward all-solution-processed large-area organic light-emitting diodes, *Adv. Mater. Technol.* 1 (2016) 1–8, <https://doi.org/10.1002/admt.201600029>.
- [3] A. Sommers, Q. Wang, X. Han, C. T'Joel, Y. Park, A. Jacobi, Ceramics and ceramic matrix composites for heat exchangers in advanced thermal systems – a review, *Appl. Therm. Eng.* (2010), <https://doi.org/10.1016/j.applthermaleng.2010.02.018>.
- [4] U.S. Mbamara, B. Olofinjana, O.O. Ajayi, C. Lorenzo-Martin, E.I. Obiajunwa, E.O. B. Ajayi, Friction and wear behavior of nitrogen-doped ZnO thin films deposited via MOCVD under dry contact, *Eng. Sci. Technol.* (2016), <https://doi.org/10.1016/j.jestch.2016.01.003>.
- [5] M. Tabandeh-Khorshid, E. Omrani, P.L. Menezes, P.K. Rohatgi, Tribological performance of self-lubricating aluminum matrix nanocomposites: role of graphene nanoplatelets, *Eng. Sci. Technol.* (2016), <https://doi.org/10.1016/j.jestch.2015.09.005>.
- [6] L. Calabrese, L. Bonaccorsi, A. Capri, E. Proverbio, Adhesion aspects of hydrophobic silane zeolite coatings for corrosion protection of aluminium substrate, *Prog. Org. Coat.* (2014), <https://doi.org/10.1016/j.porgcoat.2014.04.025>.
- [7] R. Verma, N.M. Suri, S. Kant, Effect of parameters on adhesion strength for slurry spray coating technique, *Mater. Manuf. Process.* 32 (2017) 416–424, <https://doi.org/10.1080/10426914.2016.1221090>.
- [8] R. Kromer, Y. Danlos, E. Aubignat, C. Verdy, S. Costil, Coating deposition and adhesion enhancements by laser surface texturing—metallic particles on different classes of substrates in cold spraying process, *Mater. Manuf. Process.* 32 (2017) 1642–1652, <https://doi.org/10.1080/10426914.2017.1364750>.

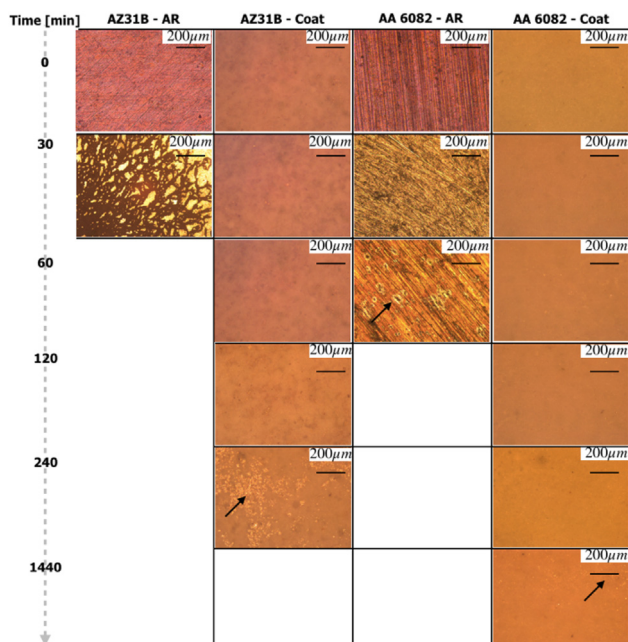


Fig. 8. Corrosion test on coated and uncoated aluminum and magnesium alloys.

- [9] X. Liu, Z. Yue, T. Romeo, J. Weber, T. Scheuermann, S. Moulton, G. Wallace, Biofunctionalized anti-corrosive silane coatings for magnesium alloys, *Acta Biomater.* (2013), <https://doi.org/10.1016/j.actbio.2012.12.025>.
- [10] P. Frontera, S. Candamano, A. Macario, F. Crea, L.A. Scarpino, P.L. Antonucci, Ferrierite zeolitic thin-layer on cordierite honeycomb support by clear solutions, *Mater. Lett.* (2013), <https://doi.org/10.1016/j.matlet.2013.03.138>.
- [11] T.F. Mastropietro, E. Drioli, S. Candamano, T. Paoletti, Crystallization and assembling of FAU nanozeolites on porous ceramic supports for zeolite membrane synthesis, *Microporous Mesoporous Mater.* (2016), <https://doi.org/10.1016/j.micromeso.2016.03.037>.
- [12] A. Matsumoto, K. Tsutsumi, K. Schumacher, K.K. Unger, Surface functionalization and stabilization of mesoporous silica spheres by silanization and their adsorption characteristics, *Langmuir* 18 (2002) 4014–4019, <https://doi.org/10.1021/la020004c>.
- [13] I. Fuke, V. Prabhu, S. Baek, Computational model for predicting coating thickness in electron beam physical vapor deposition, *J. Manuf. Process.* 7 (2005) 140–152, [https://doi.org/10.1016/S1526-6125\(05\)70091-8](https://doi.org/10.1016/S1526-6125(05)70091-8).
- [14] S. Mintova, T. Bein, Nanosized zeolite films for vapor-sensing applications, *Microporous Mesoporous Mater.* 50 (2–3) (2001) 159–166.
- [15] R.A. Munoz, D. Beving, Y. Yan, Hydrophilic zeolite coatings for improved heat transfer, *Ind. Eng. Chem. Res.* 44 (12) (2005) 4310–4315.
- [16] A.M. McDonnell, D. Beving, A. Wang, W. Chen, Y. Yan, Hydrophilic and antimicrobial zeolite coatings for gravity-independent water separation, *Adv. Funct. Mater.* 15 (2) (2005) 336–340.
- [17] Z. Li, M.C. Johnson, M. Sun, E.T. Ryan, D.J. Earl, W. Maichen, M.W. Deem, Mechanical and dielectric properties of pure-silica-zeolite low-k materials, *Angew. Chem. Int. Ed.* 45 (38) (2006) 6329–6332.
- [18] P.S. Wheatley, A.R. Butler, M.S. Crane, S. Fox, B. Xiao, A.G. Rossi, R.E. Morris, NO-releasing zeolites and their antithrombotic properties, *J. Am. Chem. Soc.* 128 (2) (2006) 502–509.
- [19] C.M. Lew, R. Cai, Y. Yan, Zeolite thin films: from computer chips to space stations, *Acc. Chem. Res.* 43 (2) (2010) 210–219.
- [20] E. Coutino-Gonzalez, W. Baekelant, B. Dieu, M.B.J. Roefsaers, J. Hofkens, Nanostructured Ag-zeolite composites as luminescence-based humidity sensors, *J. Vis. Exp.* 117 (2016), <https://doi.org/10.3791/54674> e54674.
- [21] S. Yang, J. Wang, W. Mao, D. Zhang, Y. Guo, Y. Song, G.L. Li, pH-responsive zeolitic imidazole framework nanoparticles with high active inhibitor content for self-healing anticorrosion coatings, *Colloids Surf., A* 555 (2018) 18–26.
- [22] S. Roselli, C. Deyá, M. Revuelta, A.R. Di Sarli, R. Romagnoli, Zeolites as reservoirs for Ce (III) as passivating ions in anticorrosion paints, *Corros. Rev.* 36 (3) (2018) 305–322.
- [23] N.M. Ahmed, H.S. Emira, M.M. Selim, Anticorrosive performance of ion-exchange zeolites in alkyd-based paints, *Pigm. Resin Technol.* 40 (2) (2011) 91–99.
- [24] T. Goyal, R.S. Walia, T.S. Sidhu, Study of coating thickness of cold spray process using Taguchi method, *Mater. Manuf. Process.* 27 (2012) 185–192, <https://doi.org/10.1080/10426914.2011.564249>.
- [25] M.R. Rokni, C.A. Widener, V.K. Champagne, G.A. Crawford, S.R. Nutt, The effects of heat treatment on 7075 Al cold spray deposits, *Surf. Coat. Technol.* (2017), <https://doi.org/10.1016/j.surfcoat.2016.10.064>.
- [26] W. Wan, C. Xiao, X. Zou, in: *Mesoporous Zeolites*, 2015, <https://doi.org/10.1002/9783527673957.ch13>.
- [27] G.L. Makar, J. Kruger, Corrosion of magnesium, *Int. Mater. Rev.* 38 (1993), <http://www.tandfonline.com/doi/abs/10.1179/imr.1993.38.3.138>.
- [28] J.E. Gray, B. Luan, Protective coatings on magnesium and its alloys – a critical review, *J. Alloys Compd.* (2002), [https://doi.org/10.1016/S0925-8388\(01\)01899-0](https://doi.org/10.1016/S0925-8388(01)01899-0).
- [29] P.L. Hagans, C.M. Haas, in: *Surface Engineering*, ASM International, 1994, p. 5.
- [30] C. Zhong, F. Liu, Y. Wu, J. Le, L. Liu, M. He, J. Zhu, W. Hu, Protective diffusion coatings on magnesium alloys: a review of recent developments, *J. Alloys Compd.* (2012), <https://doi.org/10.1016/j.jallcom.2011.12.124>.
- [31] K. Khanari, M. Finšgar, The corrosion inhibition of AA6082 aluminium alloy by certain azoles in chloride solution: electrochemistry and surface analysis, *Coatings* 9 (2019), <https://doi.org/10.3390/COATINGS9060380>.
- [32] Manufacturer declaration, <http://www.abcolby.com/jpaste.html>.
- [33] S. Rashmi, L. Elias, A. Chitharanjan Hegde, Multilayered Zn-Ni alloy coatings for better corrosion protection of mild steel, *Eng. Sci. Technol.* (2017), <https://doi.org/10.1016/j.jestch.2016.10.005>.
- [34] O. Lunder, B. Olsen, K. Nisancioglu, Pre-treatment of AA6060 aluminium alloy for adhesive bonding, *Int. J. Adhes. Adhes.* 22 (2) (2002) 143–150.
- [35] Y. Li, H.M. Guan, T.S. Chung, S. Kulprathipanja, Effects of novel silane modification of zeolite surface on polymer chain rigidification and partial pore blockage in polyethersulfone (PES)-zeolite A mixed matrix membranes, *J. Membr. Sci.* (2006), <https://doi.org/10.1016/j.memsci.2005.08.015>.
- [36] L. Calabrese, L. Bonaccorsi, E. Proverbio, Corrosion protection of aluminum 6061 in NaCl solution by silane-zeolite composite coatings, *J. Coat. Technol. Res.* 9 (5) (2012) 597–607.
- [37] T. Kawai, K. Tsutsumi, Reactivity of silanol groups on zeolite surfaces, *Colloid Polym. Sci.* 276 (1998) 992–998, <https://doi.org/10.1007/s003960050338>.
- [38] M. Zhou, B. Zhang, X. Liu, Oriented growth and assembly of zeolite crystals on substrates, *Chin. Sci. Bull.* 53 (6) (2008) 801–816.
- [39] D.A. Lucca, K. Herrmann, M.J. Klopffstein, Nanoindentation: measuring methods and applications, *CIRP Ann. Manuf. Technol.* (2010), <https://doi.org/10.1016/j.cirp.2010.05.009>.
- [40] F. Soltani-kordshuli, F. Zabihi, M. Eslamian, Graphene-doped PEDOT:PSS nanocomposite thin films fabricated by conventional and substrate vibration-assisted spray coating (SVASC), *Eng. Sci. Technol.* (2016), <https://doi.org/10.1016/j.jestch.2016.02.003>.
- [41] S.J. Bull, E.G. Berasetegui, Chapter 7 An overview of the potential of quantitative coating adhesion measurement by scratch testing, in: *Tribol. Interface Eng. Ser.*, 2006, [https://doi.org/10.1016/S0167-8922\(06\)80043-X](https://doi.org/10.1016/S0167-8922(06)80043-X).